

Effect of stacking order on the magnetic and transport properties of bilayer-based oxide superlattices with inversion symmetry

P. Padhan and W. Prellier

Citation: [Applied Physics Letters](#) **95**, 203107 (2009); doi: 10.1063/1.3265942

View online: <http://dx.doi.org/10.1063/1.3265942>

View Table of Contents: <http://scitation.aip.org/content/aip/journal/apl/95/20?ver=pdfcov>

Published by the [AIP Publishing](#)

Articles you may be interested in

[Effect of superconducting spacer layer thickness on magneto-transport and magnetic properties of \$\text{La}_{0.7}\text{Sr}_{0.3}\text{MnO}_3/\text{YBa}_2\text{Cu}_3\text{O}_7/\text{La}_{0.7}\text{Sr}_{0.3}\text{MnO}_3\$ heterostructures](#)

[J. Appl. Phys.](#) **115**, 013901 (2014); 10.1063/1.4861139

[Magnetic structure of \$\text{La}_{0.7}\text{Sr}_{0.3}\text{MnO}_3 / \text{La}_{0.7}\text{Sr}_{0.3}\text{FeO}_3\$ superlattices](#)

[Appl. Phys. Lett.](#) **94**, 072503 (2009); 10.1063/1.3085765

[Effect of ferromagnetic/antiferromagnetic interfaces on the magnetic properties of \$\text{La}_{2/3}\text{Sr}_{1/3}\text{MnO}_3/\text{Pr}_{2/3}\text{Ca}_{1/3}\text{MnO}_3\$ superlattices](#)

[J. Appl. Phys.](#) **99**, 08C903 (2006); 10.1063/1.2170058

[The effect of Cu-doping on the magnetic and transport properties of \$\text{La}_{0.7}\text{Sr}_{0.3}\text{MnO}_3\$](#)

[J. Appl. Phys.](#) **97**, 10H714 (2005); 10.1063/1.1860992

[Perovskite oxide tricolor superlattices with artificially broken inversion symmetry by interface effects](#)

[Appl. Phys. Lett.](#) **81**, 4793 (2002); 10.1063/1.1530734

The advertisement features a dark background with a grid pattern. On the left, there is a 3D cutaway illustration of a mechanical part with a red and yellow color gradient. The text 'Over 600 Multiphysics Simulation Projects' is prominently displayed in white and blue. A blue button with the text 'VIEW NOW >>' is located on the right. The COMSOL logo is in the bottom right corner.

Over 600 Multiphysics Simulation Projects

[VIEW NOW >>](#)

COMSOL

Effect of stacking order on the magnetic and transport properties of bilayer-based oxide superlattices with inversion symmetry

P. Padhan^{1,2} and W. Prellier^{1,a)}

¹Laboratoire CRISMAT, CNRS UMR 6508, ENSICAEN, 6 Bd du Marechal Juin, F-14050 Caen Cedex, France

²Department of Physics, Indian Institute of Technology Madras, Chennai 600036, India

(Received 8 October 2009; accepted 28 October 2009; published online 16 November 2009)

SrRuO₃-SrMnO₃ multilayers with heterointerfaces of similar inversion symmetry were fabricated. The SrTiO₃/[SrMnO₃/SrRuO₃]₁₅ multilayer shows lower Curie temperature, smaller magnetization and larger magnetoresistance compared to SrTiO₃/[SrRuO₃/SrMnO₃]₁₅ multilayer. The variations of these properties with the inversion of stacking order are well correlated with each other which occur due to pinned/biased moments and can be explained by their cumulative stress difference. © 2009 American Institute of Physics. [doi:10.1063/1.3265942]

The physical properties of the transition metal oxides observed in the structure synthesized in the form of single crystal and bulk ceramics can be significantly different when grown on a substrate due to the substrate-induced stresses. This phenomenon is widely studied using the finite size effect and a change in metal-insulator transition temperature, Curie temperature, and resistance¹ has been observed. The finite size effect is also found to be important in the engineering of interface using transition metal oxides to develop the potentially useful electronic and magnetic properties at the heterointerfaces.²⁻⁵ The superlattices with heterointerfaces build from the thin films of metal-like individual oxides show the semiconductorlike resistivity.⁶ Also some magnetic structures with heterointerfaces of the thin films of antiferromagnetic individual oxides show the ferromagnetic ordering.⁷ These systems are known with global centrosymmetry. In these systems, heterointerfaces inevitably lack spatial-inversion symmetry, as they are accompanied by asymmetric charge transfer and/or chemical potential gradient, and thereby may host novel electronic outcomes, such as electrically polar magnetic and/or metallic states.⁸ For such features to be detected by macroscopic probes, Yamada *et al.*⁹ have studied LaAlO₃/La_{0.6}Sr_{0.4}MnO₃/SrTiO₃ superlattices by breaking the inversion symmetry.

In this letter, we report a comprehensive study of multilayers SrRuO₃(SRO)-SrMnO₃(SMO) with heterointerfaces of similar inversion symmetry grown on (001) oriented SrTiO₃ (STO) substrate. In these multilayers the stacking order of the individual is reverse for example STO/SRO/SMO/SRO..... and STO/SMO/SRO/SMO..... structures. Both configurations consist of bilayers of 20 unit cells (u.c.) thick film of SRO and 5 unit cells thick film of SMO. The SRO exhibits metal-like electronic transport and ferromagnetic ordering with a Curie temperature (T_C) of ~160 K in its bulk form.¹⁰ While Cubic SMO shows insulator like electronic transport with antiferromagnetic ordering of Mn⁴⁺ below the Néel temperature (T_N) 260 K.¹¹

The STO/[(5 u.c.)SMO/(20 u.c.)SRO]_{x15} and STO/[(20 u.c.)SRO/(5 u.c.)SMO]_{x15} multilayers structures are grown by using a multitarget pulsed laser deposition system. The details of optimized deposition conditions are described

elsewhere.¹² In both the multilayer structures the top layer is 20 u.c. thick SRO. The structural characterization of these samples are performed using x-ray, while the electronic transport and magnetization measurements are performed using a physical property measurement system (Quantum Design PPMS) and superconducting quantum interference device based magnetometer (Quantum Design MPMS-5), respectively. The transport measurements are carried out by cooling the samples to the desired temperature in the absence of electric and magnetic field. While the temperature dependent magnetization and hysteresis loops are measured by cooling the sample in the presence and absence of field, respectively. The orientation of the magnetic field during the field cooled measurements remains the same. These measurements are performed in both field parallel and perpendicular to the film plane configurations.

In Fig. 1 we show the θ - 2θ x-ray scan with the 2θ range

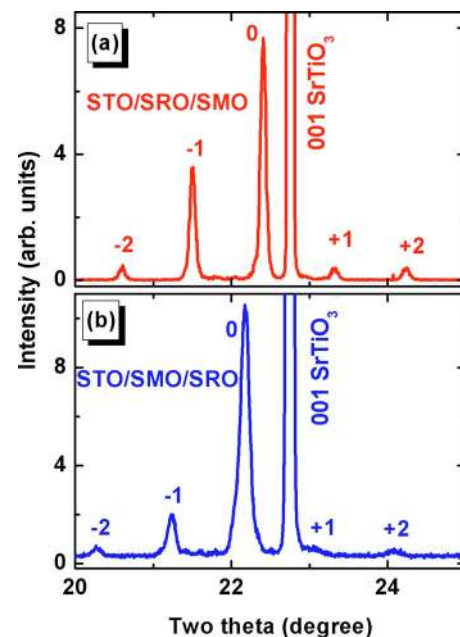


FIG. 1. (Color online) The x-ray θ - 2θ diffraction profiles around the (001) Bragg's reflection of STO of the multilayer (a) SrTiO₃/SrRuO₃/SrMnO₃ (b) SrTiO₃/SrMnO₃/SrRuO₃. The (001) Bragg's reflection of STO and several orders (0, ± 1 , ± 2 ...) of satellite peaks are indexed.

^{a)}Electronic mail: prellier@ensicaen.fr.

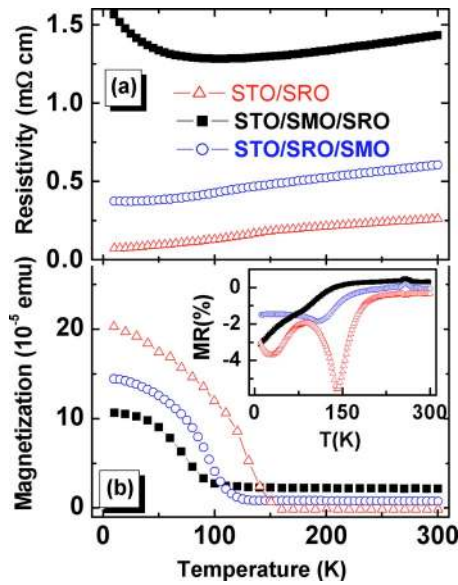


FIG. 2. (Color online) Zero-field-cooled temperature dependent resistivity (panel a), Field-cooled (0.1 tesla) temperature dependent magnetization (panel b) and temperature dependent magneto-resistance ($\{\rho(H, T) - \rho(0, T)\} / \rho(0, T) \times 100$) (inset of panel b) of 20 u.c. thick SRO (open triangle), $\text{SrTiO}_3/[\text{SrRuO}_3/\text{SrMnO}_3]_{15}$ (closed circle) and $\text{SrTiO}_3/[\text{SrMnO}_3/\text{SrRuO}_3]_{15}$ (open circle).

around (001) reflection of these two multilayer structures. The x-ray diffraction profiles show only (00l) reflections from both the film and substrate, indicating the epitaxial growth of SRO and SMO on (001)-oriented STO. In these x-ray scans the angular position of peak intensity of $\text{STO}/[\text{SMO}/\text{SRO}]_{15}$ and $\text{STO}/[\text{SRO}/\text{SMO}]_{15}$ multilayer provide their corresponding out-of-plane lattice parameter i.e., $c = 3.964$ and 4.005 Å, respectively. The observed out-of-plane lattice parameter of $\text{STO}/[\text{SMO}/\text{SRO}]_{15}$ multilayer indicates the presence +2.5% lattice mismatch with the substrate while that of the $\text{STO}/[\text{SRO}/\text{SMO}]_{15}$ multilayer indicates the presence of +1.5%. So for the observed lattice mismatch along “c” assuming volume conservation during the process of lattice distortion one can have lattice mismatch in-the-plane of $\text{STO}/[\text{SMO}/\text{SRO}]_{15}$ and $\text{STO}/[\text{SRO}/\text{SMO}]_{15}$ multilayers as -2.5% and -1.5%, respectively. However, STO provides -2.5% and +0.6% lattice mismatch in-the-plane for the epitaxial growth of SRO and SMO, respectively. Thus the observed consistency of experimental and calculated in-the-plane lattice mismatch in $\text{STO}/[\text{SMO}/\text{SRO}]_{15}$ multilayer indicates the presence of coherent modulation of *substrate-induced stress*. While the anomaly of in-the-plane lattice mismatch in $\text{STO}/[\text{SRO}/\text{SMO}]_{15}$ multilayer is due to the lattice distortion of SMO through the process of nonconservation of volume.¹² This geometrical effect at the interfaces of $\text{STO}/[\text{SMO}/\text{SRO}]_{15}$ and $\text{STO}/[\text{SRO}/\text{SMO}]_{15}$ multilayer is further analyzed from their electronic transport and magnetic properties.

Figure 2(a) shows the zero-field temperature dependent resistivity [$\rho(T)$] of the STO/SRO , $\text{STO}/[\text{SRO}/\text{SMO}]_{15}$ and $\text{STO}/[\text{SMO}/\text{SRO}]_{15}$ multilayers. The $\rho(T)$ curve of $\text{STO}/[\text{SRO}/\text{SMO}]_{15}$ multilayer is qualitatively similar to that of the 20 u.c. thick film of SRO with the anomaly at the temperature ~ 125 K. While the $\rho(T)$ at lower temperature (below ~ 105 K) shows insulatorlike behavior. Apart from

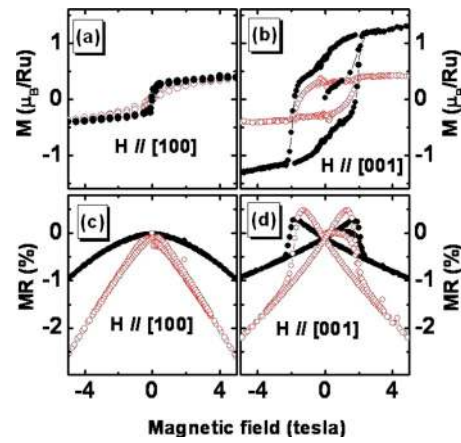


FIG. 3. (Color online) Zero-field-cooled magnetic hysteresis loop and magneto-resistance of the $\text{SrTiO}_3/[\text{SrRuO}_3/\text{SrMnO}_3]_{15}$ (sphere) and $\text{SrTiO}_3/[\text{SrMnO}_3/\text{SrRuO}_3]_{15}$ (open circle) with field parallel (panel a and c, respectively) and perpendicular (panel b and d, respectively) to the film plane.

$\rho(T)$ behavior, the magnitude of resistivity of the multilayer strongly depends on the stacking order of SRO and SMO. The in-plane resistivity of the multilayer is determined by modeling the multilayer as the parallel combinations of resistors.¹³ So irrespective of stacking order of SRO and SMO the resistivity of multilayer depends on the resistivity of the constituents and their interfaces. However, in the presence of 7 tesla field the qualitative behavior of the $\rho(T)$ is similar to that of the zero-field $\rho(T)$ with a lower magnitude of resistivity below ~ 200 K. The differences in the zero-field and in-field resistivity [i.e., $\text{MR}(\text{magneto-resistance}) = [\rho(H) - \rho(0)] / \rho(0)$] of these samples are shown in the inset of the Fig. 2(b). The high field temperature dependence MR of the multilayer compared to 20 u.c. thick film of SRO suggests the magnetic re-orientation of SRO in the multilayer. Since the MR of multilayer strongly depends on the layer stacking of SRO and SMO, we attribute magnetic re-orientation to the substrate-induced stress and *interfacial geometry*.

Figure 2(b) shows field-cooled temperature dependent magnetization [$M(T)$] of STO/SRO , $\text{STO}/[\text{SMO}/\text{SRO}]_{15}$ and $\text{STO}/[\text{SRO}/\text{SMO}]_{15}$ multilayers. The $M(T)$ measurement was performed in presence of 100 gauss out-of-plane field. The Curie temperature (T_C) of $\text{STO}/[\text{SMO}/\text{SRO}]_{15}$ and $\text{STO}/[\text{SRO}/\text{SMO}]_{15}$ multilayer (~ 97 and ~ 132 K, respectively) is relatively smaller than that of the thin film of SRO (~ 150 K). The comparison of T_C of these two multilayers indicates that the ordering of magnetic ions in SRO is more concealed in $\text{STO}/[\text{SMO}/\text{SRO}]_{15}$ multilayer than in $\text{STO}/[\text{SRO}/\text{SMO}]_{15}$ multilayer. We have further studied the zero-field-cooled magnetic hysteresis loop $M(H)$ of these samples at 10 K. The magnetic hysteresis loop of $\text{STO}/[\text{SMO}/\text{SRO}]_{15}$ and $\text{STO}/[\text{SRO}/\text{SMO}]_{15}$ multilayers are compared in the Figs. 3(a) and 3(b) for field oriented along the [100] and [001] directions of SrTiO_3 , respectively. The maximum value of magnetization of $\text{STO}/[\text{SRO}/\text{SMO}]_{15}$ multilayer for field oriented along the [100] and [001] directions of SrTiO_3 is $\sim 0.4 \mu_B/\text{Ru}$ and $1.3 \mu_B/\text{Ru}$ at 4.5 T, respectively. The observed variation of magnetization of $\text{STO}/[\text{SRO}/\text{SMO}]_{15}$ multilayer with the orientation of fields is studied for a series of multilayers in

details and attributed to pinned/biased moments at the interfaces.¹⁴ However, as the stacking order of the SRO and SMO is changed (i.e., for STO/[SMO/SRO]₁₅ multilayer) the magnetization at 4.5 T field is $\sim 0.39 \mu_B/\text{Ru}$ (significantly lower than the theoretical value $\sim 1.6 \mu_B/\text{Ru}$),¹⁵ which is independent of orientation of fields. So, the magnetization of SrRuO₃ in the SRO-SMO multilayer for field along the [100] direction of SrTiO₃ is independent of stacking order of SRO and SMO while it is strongly dependent of stacking order for field along the [001] direction of SrTiO₃. For field along the [001] direction of SrTiO₃ the presence of soft pinned/biased moments in STO/[SRO/SMO]₁₅ multilayer in contrast to the very hard pinned/biased moments in STO/[SMO/SRO]₁₅ multilayer is attributed to the lattice distortion of SMO through the process of nonconservation.¹² Though there is a significant decrease of magnetization of SRO in STO/[SMO/SRO]₁₅ multilayer its magnetic easy axis is remain same. Hence the magnetic easy axis of SRO-SMO multilayer is independent of stacking order of SRO and SMO.

We have also measured magnetic field dependent resistivity $\rho(H)$ of these multilayers and calculated their MR at 10 K. The field dependent MR (MR-H) of two multilayers are compared in Figs. 3(c) and 3(d) for field oriented along the [100] and [001] directions of SrTiO₃, respectively. The MR of STO/[SRO/SMO]₁₅ multilayer is suppressed compared to single layer SRO film on STO.¹⁶ While MR of STO/[SMO/SRO]₁₅ multilayer for field oriented along the [100] ([001]) direction of SrTiO₃ is suppressed (enhanced) compared to single layer SRO film on STO. However, the MR of STO/[SMO/SRO]₁₅ multilayer is larger compared to the MR of STO/[SRO/SMO]₁₅. Even though the observed MR-H is the cumulative effect of interfaces and top-conducting layer SRO, the MR-H curve of these multilayers strongly depend on the stacking order of SRO and SMO. The enhanced MR of STO/[SMO/SRO]₁₅ multilayer for field along [001] direction of SrTiO₃ is consistent with the observed lower magnetization [Fig. 3(b)]. The lower magnetization of STO/[SMO/SRO]₁₅ indicates presence of pinned/biased moments^{14–17} which facilitates more spin-dependent scattering¹⁸ compared to of STO/[SRO/SMO]₁₅ multilayer. The presence of more spin dependent scattering is responsible for higher resistance and hence higher MR of STO/[SRO/SMO]₁₅ multilayer for field along [001] direc-

tion of SrTiO₃. Note that the electronic transport for these multilayers strongly depends on tunneling,¹⁹ spin dependent scattering¹⁸ and interfacial scattering.

In conclusion, we have studied the SrRuO₃-SrMnO₃ multilayers with heterointerfaces of similar inversion symmetry. The inversion symmetry is driven by a significant cumulative stress difference with the inversion of stacking order of SrRuO₃-SrMnO₃. We observed lower T_C, smaller magnetization and larger MR in STO/[SMO/SRO]₁₅ multilayer compared to STO/[SRO/SMO]₁₅ multilayer. The variations of these properties are well correlated with each other which occur due to pinned/biased moments and can be explained by their cumulative stress difference. These findings are of high importance for a detailed control of the growth of oxide-based multilayers.

Support of Indo-French Center CEFIPRA/IFPCAR, C'Nano, and STAR program is acknowledged.

- ¹D. Toyota, I. Ohkubo, H. Kumigashira, M. Oshima, T. Ohnishi, M. Lippmaa, M. Kawasaki and H. Koinuma, *J. Appl. Phys.* **99**, 08N505 (2006).
- ²C. H. Ahn, S. Gariglio, P. Paruch, T. Tybell, L. Antognazza, and J.-M. Triscone, *Science* **284**, 1152 (1999).
- ³H. Yamada, Y. Ogawa, Y. Ishii, H. Sato, H. Akoh, M. Kawasaki, and Y. Tokura, *Science* **305**, 646 (2004).
- ⁴P. Murugavel, P. Padhan, and W. Prellier, *Appl. Phys. Lett.* **85**, 4992 (2004).
- ⁵W. C. Sheets, B. Mercey, and W. Prellier, *Appl. Phys. Lett.* **91**, 192102 (2007).
- ⁶A. Venimadhav, M. S. Hegde, R. Rawat, I. Das, P. L. Paulose, and E. V. Sampathkumaran, *Phys. Rev. B* **63**, 214404 (2001).
- ⁷P. Padhan and W. Prellier, *Phys. Rev. B* **72**, 094407 (2005).
- ⁸J. Matsuno, Th. Lottermoser, T. Arima, M. Kawasaki, and Y. Tokura, *Phys. Rev. B* **75**, 180403(R) (2007).
- ⁹H. Yamada, M. Kawasaki, Y. Ogawa, and Y. Tokura, *Appl. Phys. Lett.* **81**, 4793 (2002).
- ¹⁰G. Cao, S. McCall, M. Shepard, J. E. Crow, and R. P. Guertin, *Phys. Rev. B* **56**, 321 (1997).
- ¹¹T. Takeda and S. Ohara, *J. Phys. Soc. Jpn.* **37**, 275 (1974).
- ¹²P. Padhan, W. Prellier, and B. Mercey, *Phys. Rev. B* **70**, 184419 (2004).
- ¹³P. Padhan and R. C. Budhani, *Phys. Rev. B* **67**, 024414 (2003).
- ¹⁴P. Padhan and W. Prellier, *Phys. Rev. B* **72**, 104416 (2005).
- ¹⁵D. J. Singh, *J. Appl. Phys.* **79**, 4818 (1996).
- ¹⁶P. Padhan and W. Prellier, *J. Appl. Phys.* **98**, 083906 (2005).
- ¹⁷Y. Choi, Y. Z. Yoo, O. Chmaissem, A. Ullah, S. Kolesnik, C. W. Kimball, D. Haskel, J. S. Jiang, and S. D. Bader, *J. Appl. Phys.* **103**, 07B517 (2008).
- ¹⁸*Ultrathin Magnetic Structures II*, edited by B. Heinrich and J. A. C. Bland (Springer, Berlin, 1994).
- ¹⁹J. S. Moodera and G. Mathon, *J. Magn. Magn. Mater.* **200**, 248 (1999).